Desalination and Water Treatment
www.deswater.com

doi: 10.1080/19443994.2015.1044475

57 (2016) 10995–11007
May

Taylor & Francis
Taylor & Francis Group

Performance assessment of synthesized CNT/polypropylene composite membrane distillation for oil field produced water desalination

Khaled Okiel[a], Abdel Hameed M. El-Aassar[b], Tarek Temraz[c], Salah El-Etriby[c], Hosam A. Shawky[b,*]

[a]*Gemsa Petroleum Company, New El-maadi, Cairo, Egypt, Tel. +201002553048; email: khaledmazher@yahoo.com*
[b]*Egyptian Desalination Research Center of Excellence EDRC, Desert Research Center, El-Matariya, P.O.B 11753, Cairo, Egypt, Tel. +2 01002501524; email: hameed_m50@yahoo.com (A.H.M. El-Aassar), Tel. +2 01002930710; Fax: +2 0226389069; email: hashawky@EDRC.gov.eg (H.A. Shawky)*
[c]*Faculty of Science, Suez Canal University, Egypt, Tel. +201148866440; email: ttemraz@yahoo.com (T. Temraz), Tel. +201001545863; email: s_eletreby@yahoo.com (S. El-Etriby)*

Received 6 September 2014; Accepted 10 April 2015

ABSTRACT

Multi-walled carbon nanotubes (MWCNTs)/polypropylene (PP) blend membranes were synthesized by phase inversion process, using xylene as a solvent and methyl isobutyl ketone (MIBK) as a dispersion medium for MWCNTs. The prepared MWCNTs/PP membranes were characterized using several analytical techniques such as: attenuated total reflections Fourier transform infrared spectroscopy, contact angle measurement, atomic force microscope (AFM), and scanning electron microscope (SEM). Performance of the synthesized membranes in vacuum-enhanced direct contact membrane distillation (VEDCMD) process was evaluated using 55˚C feed synthetic water and/or oil field produced water samples with salinities up to 230,000 ppm. Effect of membrane preparation conditions, including polymer concentration, polymer thickness, and CNT concentrations as well as operating temperatures and streams flow rates on the flux were studied. The results showed an improvement in membranes characteristics and trans-membrane flux by MWCNTs addition. Contact angle measurements indicate that the hydrophobicity of MWCNT/PP membrane was significantly increased compared to the pure PP membrane. The SEM images showed a well dispersion of MWCNTs in the PP matrix. By analyzing AFM images, the roughness parameters and mean pore size increase by either using MIBK or decreasing PP polymer concentration. On the other hand, by blending MWCNTs, the roughness parameters increase with decreasing of mean pore size. The salt rejection of the synthesized membranes was greater than 99.9%. The results show that MWCNTs enhanced the performance of VEDCMD with 58% at the same operating conditions. The obtained flux ranged from 45.95 to 19.66 L/m^2 h, using 10,000 ppm and brine oil field produced water, respectively, by MWCNT/PP nano-composite membrane with 5 mg/g of MWCNTs and thickness 50 μm.

Keywords: PP/MWCNTs; Composite membrane distillation; Water desalination

*Corresponding author.

1. Introduction

In crude oil producing operations, it is often necessary to handle brine that is produced with the crude oil. This brine must be separated from the crude oil and disposed off in a manner that does not violate environmental criteria. In offshore areas, the governing regulatory body specifies maximum dissolved solids content in water that is allowed to be discharged overboard [1]. The Egyptian environmental law stipulates that disposed water should not contain 2,000 ppm of dissolved solids more than the TDS of the disposed surface water, and this requirement is becoming more enforced as damaging environmental effects from oily wastewater become more apparent. The regulations require that non-dissolved and dissolved components should be removed from the wastewater before disposal [2]. Desalination of oil field produced water can potentially provide a new source of water and will remove the hazards of oil field effluents on environment.

Water desalination is attracting more and more interest and attention, as they are most important methods to solve the problem of water shortage. Desalination can be achieved using different techniques. Industrial desalination technologies can be classified into two categories: (i) phase-change or thermal processes; include multi-stage flash (MSF) distillation, multiple effect boiling, and vapor compression; (ii) membrane filtration processes include reverse osmosis (RO) and electro dialysis [3]. RO and MSF distillation are the most frequently used techniques for desalination of brackish water and seawater.

During the past years, membrane distillation (MD) has emerged as an attractive and competitive alternate technique [4–18] especially for high concentrated feed solutions or brines [19,20].

MD is a thermally driven separation process, in which only vapor is transported through a porous hydrophobic membrane. The driving force in MD is the vapor pressure difference induced between both membrane sides. Different configurations have been considered to apply this driving force such as (i) direct contact membrane distillation, (ii) sweeping gas membrane distillation, (iii) vacuum membrane distillation, and (iv) air gap membrane distillation. MD can be used for various applications (desalination, environmental/waste cleanup, water-reuse, food, medical, etc.) [4].

MD has many advantages such as: (1) gives 100% (theoretical) rejection of ions, macromolecules, colloids, cells, and other nonvolatiles, (2) highly concentrated salt solutions can easily be treated, (3) lower operating temperatures than conventional distillation, (4) lower operating pressures than conventional pressure-driven membrane separation processes, and (5) reduced vapor spaces compared to conventional distillation processes [8].

Direct contact membrane distillation (DCMD) is the simplest MD configuration and is widely employed in desalination of seawater and brackish waters, in DCMD, the hot solution (feed) is in direct contact with the hot membrane side surface. Therefore, evaporation takes place at the feed-membrane surface. The vapor is moved by the pressure difference across the membrane to the permeate side and condenses inside the membrane module. Because of the hydrophobic characteristic, the feed cannot penetrate the membrane (only the gas phase exists inside the membrane pores) [9,13,21–27].

A desirable DCMD membrane providing a high flux, high long-term stability, and high energy efficiency is known to require characteristics such as high bulk and surface porosities, optimum pore size and pore size distribution, high degree of pores interconnectivity, high hydrophobicity, low thermal conductivity, and an optimum thickness [5,8]. In the membrane distillation literature, commercial hydrophobic microfiltration and ultrafiltration membranes have been commonly applied by researchers but they do not necessarily meet all of the above-mentioned characteristics as they have been designed and fabricated for other processes rather than DCMD. The pore size of the membranes frequently used in MD lies between 10 nm and 1 μm, and the porosity should be as high as possible. It is generally admitted that the MD permeate flux increases with increase in pore size and/or porosity. The choice of a membrane for MD applications is a compromise between a low heat transfer flux by conduction achieved using thicker membranes and a high permeate flux achieved using thin membranes having large pore size, low pore tortuosity, and high porosity. Since the hydrophobic character of the membrane is a crucial requirement in MD, membranes have to be made by materials with low values of surface energy. Hydrophobicity can be achieved by either using hydrophobic materials or making the hydrophilic membrane surface energy as low as possible, applying different surface modification techniques [4].

The performance of DCMD can be improved in different ways. One of them is vacuum-enhanced direct contact membrane distillation (VEDCMD), the cooler water stream flows under negative pressure (vacuum). Under specific operating conditions, VEDCMD has been shown to increase flux by up to 85% compared to the conventional DCMD configuration [15–17].

Carbon nanotubes (CNTs) were used to increase the hydrophobicity of membranes. Also, the MWCNTs enhance the roughness of surfaces results in highly super-hydrophobic membrane [28]. CNT membranes could successfully operate in DCMD for synthetic seawater desalination [29,30].

This study focuses on the synthesis of MWCNTs/polypropylene composite membrane via dry-casting process using dispersion medium (methyl isobutyl ketone) to avoid MWCNTs aggregation. Moreover, the present work aims to enhance the performance of the synthesized membranes for high saline oil field produced water desalination by optimizing DCMD conditions. The prepared membranes were characterized using attenuated total reflections Fourier transform infra-red (ATR-FTIR), contact angle measurement, scanning electron microscope (SEM) and atomic force microscope (AFM). The influence of membrane preparation conditions and operating conditions onto the membrane performance in VEDCMD process was evaluated. The VEDCMD experiments were achieved using a novel pilot-scale MD unit. The feed water was synthetic NaCl solution with different salinities. After that, the applicability of the synthesized membranes was conducted using natural oil field produced water sample with salinity 230,000 ppm collected from the area located in Gemsa oil field in the Eastern desert, Egypt.

2. Experimental

2.1. Materials

Polypropylene (PP) homo-polymer (H030SG), having melt flow rate of 11 g/10 min and melting point 161˚C, supplied by Exxonmobil Chemical company was used in this work. PP was dissolved in Xylene (L.R. grade, International Chemicals). Multi-walled carbon nanotubes (MWCNTs) was supplied from Nano-Tech Egypt for Photo-Electronics, Egypt, with purity of 95 wt.%. Fig. 1 shows TEM micrograph of MWCNTs using High-Resolution Transmission Electron Microscope (HRTEM): JEM-2100, where the average outer diameter is 10 ± 2 nm and inner diameter 2 ± 0.4 nm and lengths >660 nm. In this work, methyl isobutyl ketone (MIBK), analytical standard grade, from Aldrich was used as MWCNT dispersion medium to avoid MWCNT aggregation.

2.2. Preparation of hydrophobic polypropylene membrane using phase inversion method

Casting solution was prepared by dissolving a specific weight of PP using xylene as a solvent which was added to a 500-ml beaker. In a heating mantle, the casting solution was heated to around 130˚C with stirring at 320 rpm until PP was completely dissolved and a clear solution was obtained. Then, the polymer solution was cast over heated glass plate Petri dish with diameter 100 mm at 118˚C. The cast films were exposed to solvent evaporation for a predetermined time 60 min. The solvent was allowed to evaporate until a gel membrane was obtained. The resulting membrane was immersed in hot water (at 80˚C) for three hours to remove excessive solvent. The resulted membrane (100 mm diameter) was stored in distilled water for the measurements of membrane characterization and performance experiments.

2.3. Preparation of MWCNTs/polypropylene composite membrane

Different weights of MWCNTs were placed in 10 ml MIBK, which used as a dispersion medium with continues stirring at 450 rpm for 24 h [31]. After that, casting solution previously prepared in step 2.2 was added with continuous stirring. The solution was then casted on a glass plate Petri dish with diameter 100 mm in an oven with temperature 118˚C. Different membranes were then obtained after 15 min. The resulting membranes were immersed in hot water (at 80˚C) for 3 h to remove any excessive solvent and stored in distilled water for further investigation.

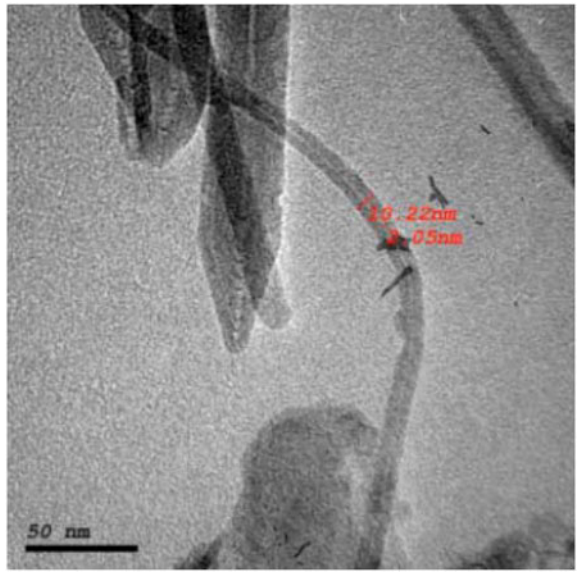

Fig. 1. TEM micrograph of MWCNTs.

2.4. Membrane characterization

Membranes used for the chemical and surface morphological analysis were washed with deionized water and dried under vacuum.

Characterization of functional groups of the synthesized membranes was done by Fourier transform infrared ATR-FTIR spectroscopy (Nicolet 8700, Thermo-Scientific, USA) with an attenuated total reflection (ATR) unit (ZnSe crystal, 45°). IR spectra of the membranes were recorded in transmittance mode over a wave number range of 4,000–650 cm^{-1} at 25°C.

Water contact angle (WCA) was measured using a contact angle instrument (Dataphysics OCA15EC, Germany) by the sessile drop method. Deionized water was used as the probe liquid in all measurements, and the contact angles between water and the membrane surface were measured for the evaluation of the membrane hydrophobicity/hydrophilicity. The volume of the water droplet used in the measurement was 2 μL. Five different positions on the membrane surface were measured to determine the average value of WCA.

Surface morphology of the membranes was studied with a SEM Model Quanta SEM (FEI Company) at 5 kV. For the cross section images, samples of the membranes were frozen in liquid nitrogen and fractured. After sputtering with gold, they were viewed with a SEM Philips microscope at 30 kV.

Also, the surface morphology of the membranes was characterized by tapping mode atomic force microscope (TM-AFM) on a Nano-scope III equipped with 1553D scanner from Digital Instruments, Santa Barbara, CA, USA. Small pieces of approximately 0.5 × 0.5 cm in area were cut from each membrane and fixed over a magnetic holder by using double side adhesive tape. All the TM-AFM images were made in air at room temperature at different locations of each membrane sample. In this study, scans were made on areas of 5 × 5 μm and areas of 2 × 2 μm were selected randomly on the membrane surface for analysis. Roughness parameters and pore sizes as well as the nodule sizes were measured through TM-AFM images analysis that was done using Gwyddion 2.34 computer program. This AFM software program allows quantitative determination of pores or nodules by use of the images in conjunction with digitally stored line profiles. The pore diameters were determined for a minimum of 28 pores on each membrane sample.

2.5. The VEDCMD experimental setup

The VEDCMD experimental setup is schematically depicted in Fig. 2 [15–17]. The membrane cell consisted of two compartments, the feed side and the permeate side. The compartments were made of polyacrylic to resist corrosion by NaCl solutions. The module positioned horizontally so that the feed solution flowed through the bottom compartment of the cell while the cooling water passed through the upper compartment. The feed and permeate separated by the hydrophobic porous membrane. The effective area of the membrane was 0.0018 m^2. A cooler (handmade water cooler with power 0.55 kW) was used for the regulation of the cold stream temperature, and a thermostatic hot feed water bath was used for the regulation of the hot stream temperature, two flow meters were used (LIQUI-VIEW model FLM21–10 with measuring range 2.8–45 L/min) for the regulation of the flow rate of the two streams meanwhile two centrifugal pumps (the cold pump 135 w, the hot pump 300 w) and two manometers (WSG-SOLO model 100 mm radial manometer with pressure range from −30 to 70 psi) were used for registering the module inlet pressures of the two streams, also four thermocouples (accuracy ± 0.1°C) for evaluating the module inlet and outlet temperatures of both streams. The volume tank of the hot stream and cold stream was of 15 and 10 L, respectively. The feed and cold solutions were contained in double-walled reservoirs and circulated through the membrane module using centrifugal pumps. Where the cold centrifugal pump installed to drown the cold stream to reduce the pressure (P pore) in the membrane pores as shown in Fig. 2. The outlet temperatures of the hot and cold sides were continually monitored and recorded. The permeated liquid was circulated through a graduated cylinder, and the volume measured at regular intervals. All data were obtained from the prepared membranes with stable flux, and the reported flux is the mean value measured every hour over a 4–6 h period. The purity of the water extracted was determined through water conductivity using an electrical conductivity meter (EC470-L, ISTEK, Korea), and it should be noted here that any increase in permeate conductivity indicates that liquid water passes through the membrane so that result is rejected, in other words, the salt rejection of all membranes was 99.99%.

In order to check the presence of leakages in the system, as well as the membrane hydrophobicity, the volume in the graduated cylinder was observed when only the hot stream was recirculated for at least 30 min before starting the experiment. Then, each experiment was initiated only when no variation was reported on the display for the time of observation. During the experiments, the feed was at atmospheric pressure and its flow rate was varied between 6 and

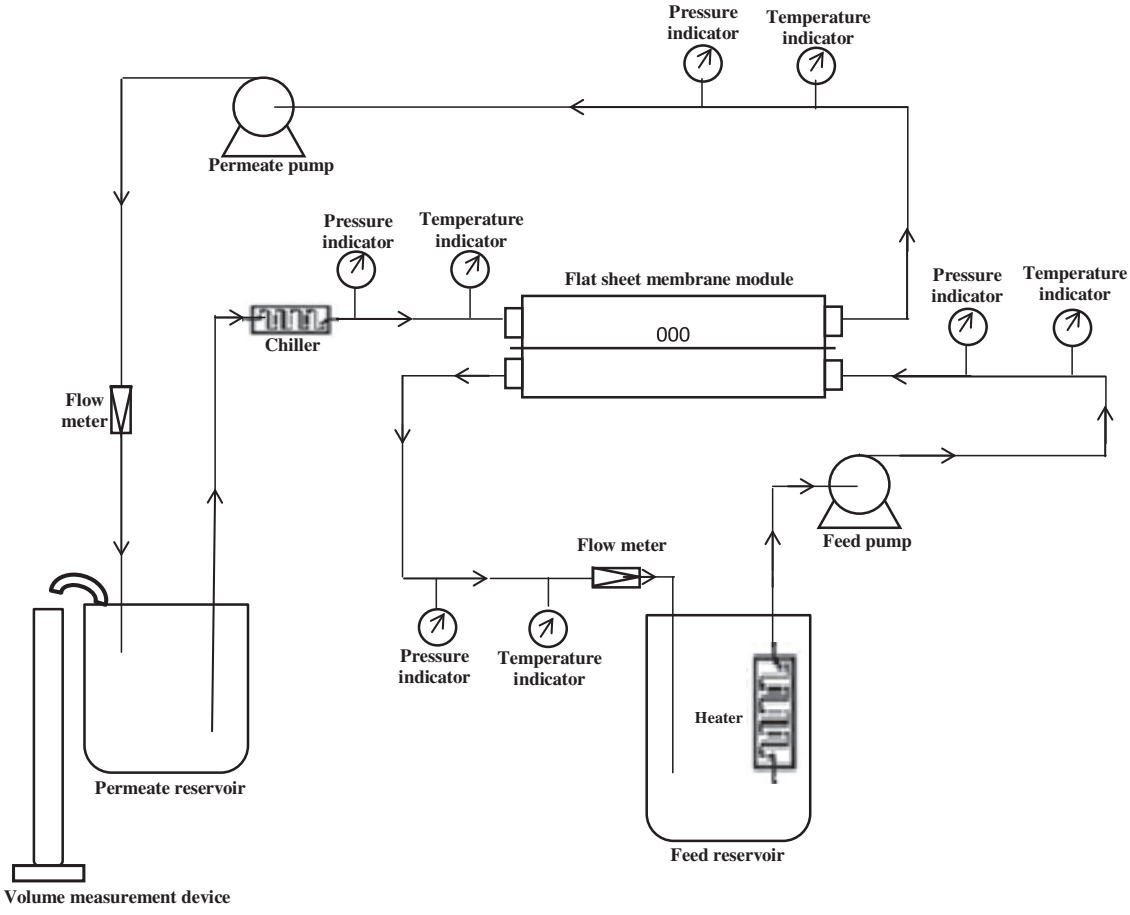

Fig. 2. Diagram of direct contact membrane distillation experimental unit.

15 L/min, while the feed temperature was varied between 40 and 60°C. In VEDCMD tests, the distillate flow rate was kept at about 6 L/min with negative pressure −3 psi and the distillate temperature was in the range of 13–14°C.

2.6. Feed water samples

The synthetic feed water used in the preliminary tests had different salinities ranged from 10,000 to 230,000 ppm of NaCl. On the other hand, the oil field produced wastewater samples with (TDS 230,000 mg/l) was collected from the main effluent wastewater pipeline after wastewater treatment unit before disposal. That oil field belongs to Gemsa Petroleum Company located in Eastern Desert of Egypt. The general characteristics of produced water were carried out in the Egyptian Petroleum Research Institute, Analysis and Evaluation department, central laboratory, and the results of crude oil and produced water are given in Table 1.

Table 1
Chemical composition of wastewater (after wastewater treatment plant treatment)

Constituents	Results
Total dissolved solids	231985 ppm
Conductivity	21.2×10^{-2} mhos/cm at 22.5°C
Density	1.15819 g/ml
Oil in water	5.0 ppm

3. Results and discussion

To improve the performance of PP membranes in DCMD process, blending with MWCNTs was done using MIBK as a dispersion solution. The characterization of the prepared, modified, and non-modified PP membranes was achieved using different techniques. After that, the performance for all membranes was evaluated to study the effect of different parameters that may affect on trans-membrane flux and to make a comparison study.

3.1. Characterization of membranes

The characterization of synthetic membranes was carried out through ATR-FTIR spectroscopy, contact angle measurement, and change in surface morphology by SEM and AFM.

3.1.1. ATR-FTIR spectroscopy

The interactions at the PP matrix/MWCNTs interface influence the vibrational spectrum of chromophore groups, even if the content of MWCNTs is insignificant. This could be seen from the behavior in the IR absorption as shown in Fig. 3.

The noticeable absorption bands at 840 and 998 cm^{-1} are characteristic for the bending vibrations in the crystalline phase. With increasing MWCNTs content, the intensity of these absorption bands grows, indicating the incorporation of helical segments into the crystal lattice and an increase in the number of chains consisting of the alternating trans-gauche conformers. Furthermore, the intensity of methyl groups pendulum swings near 600 cm^{-1} changes, as well as near 1,550 and 1,639 cm^{-1} [32]. That also shows a change in the interaction nature between the molecular chains, which possibly is realized through their bonds with MWCNTs.

3.1.2. Contact angle measurement

Contact angle measurement is the quantitative indicator of changing the membrane surface hydrophobicity. The results in Table 2 indicate that the hydrophobicity of MWCNT/PP membrane is significantly increased compared to neat PP membrane. These results confirm that the addition of non-functionalized MWCNT increases the hydrophobicity of the composite membrane [28,37].

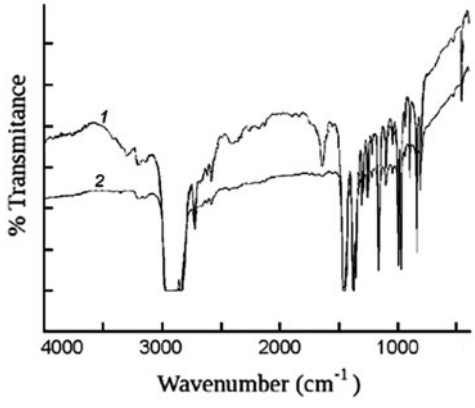

Fig. 3. FT-IR spectra for (1) the neat PP membrane, MWCNT/PP membrane with and (2) 5 (mg/g) MWCNTs.

3.1.3. SEM characterization

Figs. 4 and 5 show the SEM photographs of the surfaces for both neat PP and MWCNTs/PP blend membranes, respectively. The PP membrane modified by MWCNTs looks to have higher surface roughness compared with that of neat PP membrane. From the cross section SEM image for MWCNTs/PP membrane (Fig. 6), it can be seen that MWCNTs are well homogenously mixed and evenly distributed throughout the polymer matrix.

3.1.4. AFM characterization

The AFM photographs of the surfaces for MWCNTs/PP blend membrane show more roughness nodule aggregates compared to neat PP membrane (Figs. 7 and 8). In AFM image, the nodules are seen as bright high peaks, whereas the pores are seen as dark depressions.

Among the different parameters that have main impact on the membrane performance in VEDCMD process, there are two important parameters related to membrane characteristics. These two parameters are the surface roughness and mean pore size. By increasing the surface roughness, the surface area increases and trans-membrane flux increases. On the other hand, the mean pore size must be small as possible to avoid the membrane wetting. Table 2 shows the different roughness parameters and mean pore size of different synthesized membranes. It was found that the roughness parameters and mean pore size increase by either using MIBK or decreasing PP polymer concentration. On the other hand, by blending MWCNTs, the roughness parameters increase with decreasing mean pore size. The modification of PP membrane with MWCNTs will predict to improve the membrane performance due to MWCNTs effectively restrains the macro-voids in the membrane [33,36].

3.2. Membrane distillation performance evaluation

The effect of membrane preparation conditions such as polymer concentration, polymer thickness, and CNT concentrations as well as operating temperatures and streams flow rates on the flux was studied to investigate the optimum preparation conditions that give the best performance. It is important to mention that most synthesized membranes have salt rejection (%) higher than 99.9.

Table 2
Contact angle, roughness parameter, and mean pore size of some prepared membranes

Sample	Contact angle (°)	Mean roughness (ra) nm	Mean pore size nm
Neat P·P with 2.5 wt.%	108	37	453
Neat P·P with 1.9 wt.%	108	118	1,214
P·P with MIBK without CNT	110	108	1,319
P·P with MIBK with CNT 5 mg/g	118	180	846

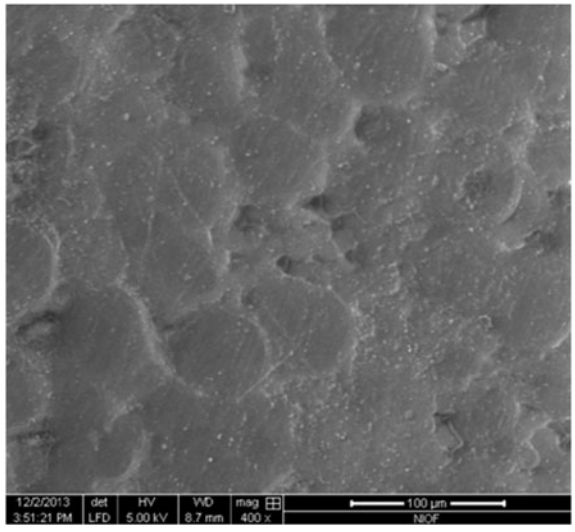

Fig. 4. SEM of neat PP surfaces membrane with polymer concentration 2.5 wt.%.

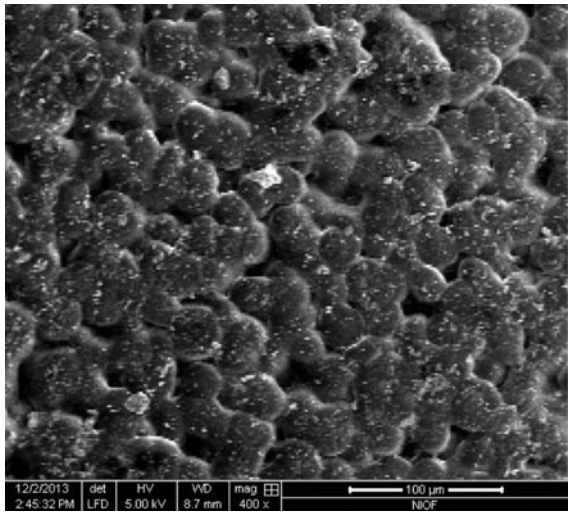

Fig. 5. SEM of MWCNTs/PP nano-composite membrane with 2.5 mg/g MWCNTs.

3.2.1. Effect of operating conditions

3.2.1.1. Feed temperature. Fig. 9 shows the relation between the trans-membrane flux and feed temperature for neat PP membrane with 50 µm thickness and polymer concentration 2.5 wt.%. The experiments were tested at hot side flow rate was 12 L/min, the cold side flow rate was 6 L/min, and the NaCl feed water TDS was 10,000 ppm.

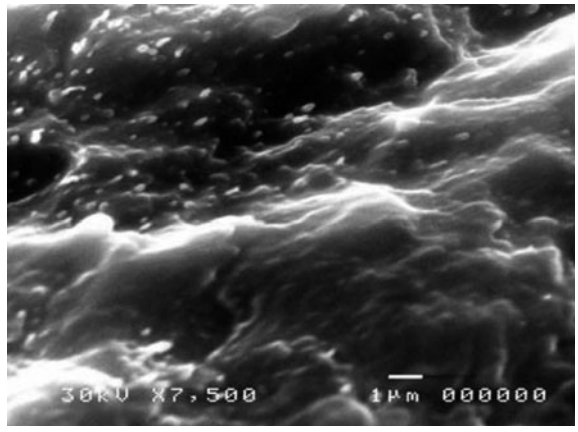

Fig. 6. Cross-sectional SEM of MWCNTs/PP nano-composite membrane with 5 mg/g MWCNTs.

The results showed that the feed water temperature increased from 45 to 60C and the trans-membrane flux increased from 8.63 to 39.42 L/m^2 h. This can be attributed to the exponential increase of the vapor pressure of the feed aqueous solution with temperature, which enhances the driving force. Also, the membrane heat transfer coefficient and the membrane mass transfer coefficient increase as the temperature increased [11,21].

3.2.1.2. Feed flow rate

Effect of feed flow rate on the permeate flux of neat PP membrane of 50 µm thickness and polymer concentration of 2.5 wt.% was studied as shown in Fig. 10. The experiments were tested at hot side temperature 55C with TDS 10,000 ppm. On the other hand, the cold side flow rate was 6 L/min. The results show that increasing in the feed flow rate from 6 to 15 L/min increases the trans-membrane flux from 8.20 to

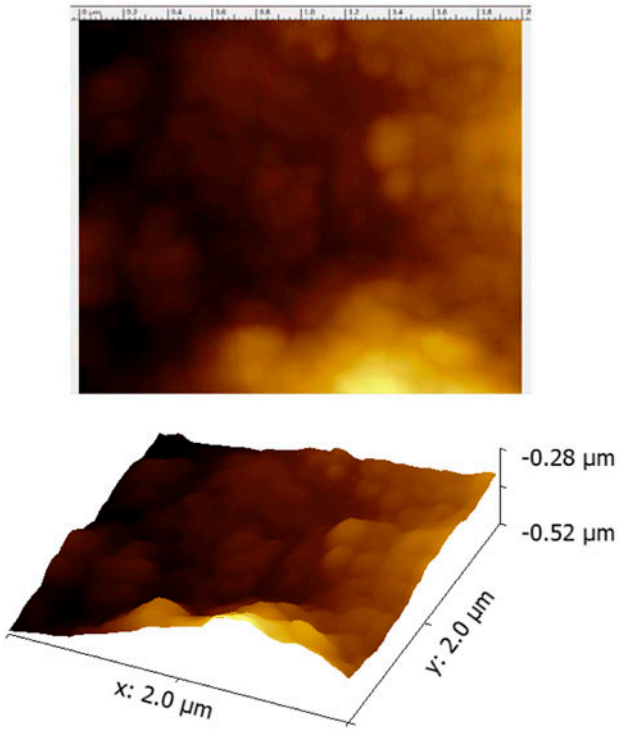

Fig. 7. AFM photographs of surface and 3D of neat PP membrane with polymer concentration 2.5 wt.%.

34.52 L/m^2 h. This is due to increasing volumetric flow rate which will enhance the permeate flux. The fluid velocity rises when the volumetric flow rates

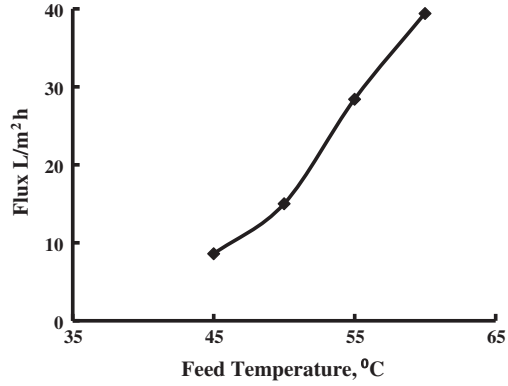

Fig. 9. The effect of feed temperature on flux.

increase, so that the convective heat transfer coefficient develops and the thermal boundary layer thickness decreases. As a result, the temperature polarization effect reduces [13,27].

3.2.1. Effect of membrane preparation conditions

From the aforementioned studies on the performance of different operating conditions and according to manufacture feed pump manual, the feed flow rate was selected to be 12 l/min with feed temperature 55C for the effect of membrane preparation condition on the permeate flux studies.

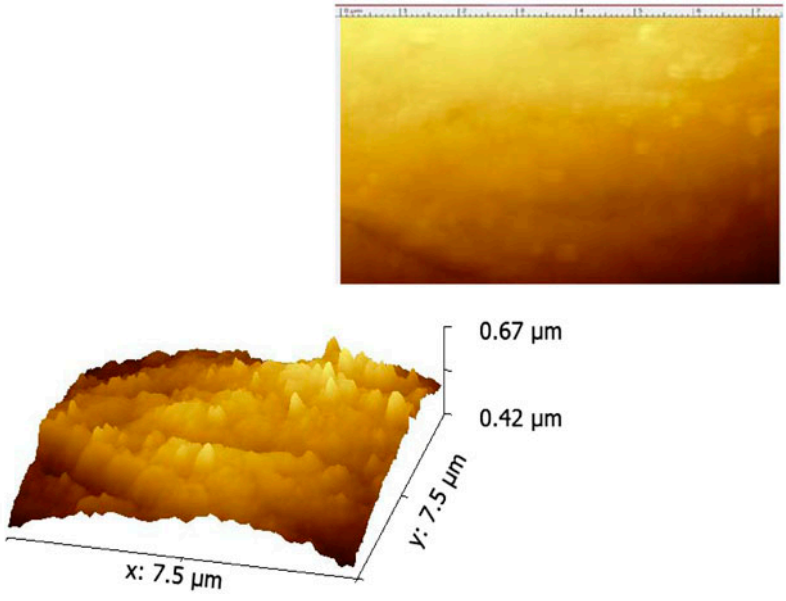

Fig. 8. AFM photographs of surface and 3D of MWCNTs/PP nano-composite membrane with 2.5 mg/gm MWCNTs.

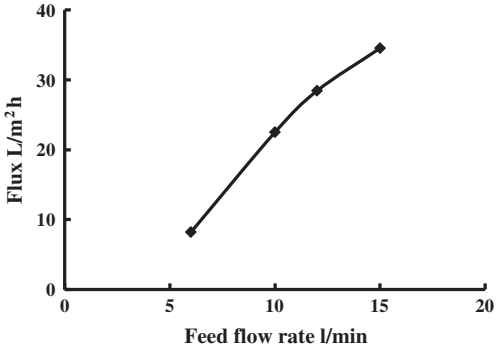

Fig. 10. The effect of feed flow rate on flux.

3.2.1.1. Polymer concentration. Effect of polymer concentration on the membrane performance was studied as shown in (Table 3). Different polymer concentrations ranged from 1.9 to 5 wt.% were used to prepare different MD with same thickness of 50 μm. These experiments were performed using synthetic feed water of 10,000 ppm NaCl. The temperature of both feed and permeate was 55 and 15˚C, respectively.

It is obvious that, as the polymer concentration decreases the trans-membrane flux increases, this is attributed to the increase in pore size and porosity (based on the AFM results) by decreasing the polymer concentration until 2.5 wt.%. By further decreasing the polymer concentration 1.9 wt.%, the feed water penetrated into the pores and a consequent pore-wetting phenomenon is occurred. This could be explained by the formation of membrane with large pores [10,25].

3.2.1.2. PP membrane thickness

Fig. 11 illustrates the effect of PP membrane thickness on the DCMD performance. Four membranes of neat PP with constant polymer concentration (2.5 wt.%) and different thickness ranged from 40 to 130 μm were prepared. These experiments were performed with feed and permeate temperatures of 55 and 15˚C, respectively, and feed salt concentration of 10,000 ppm NaCl. The results indicate that trans-membrane flux decreased from 33.12 to 5.63 L/m^2 h with increasing the membrane thickness from 40 to 130 μm. This result confirms that there is an inversely proportional relationship between the membrane thickness and the permeate flux, i.e. the permeate flux is reduced as the membrane becomes thicker, because the mass transfer resistance increases [8].

3.2.3. MWCNT content in PP matrix

Different MWCNTs concentrations ranged from 2 to 20 mg/g were used to prepare series of PP nano-composite membranes with the same membrane thickness of 50 μm and PP concentration 2.5 wt.% to explore the effect of MWCNTs on the membrane performance, as shown in (Table 4). These experiments were performed with feed and permeate temperatures of 55 and 15˚C, respectively, where the feed and permeate flow rates were 12 and 6 L/min respectively and feed salt concentration of 10,000 ppm NaCl solution. The salt rejections (%) of acceptable results were greater than 99.9%.

From Table 4, it is obvious that MWCNTs prevented the pore-wetting phenomenon which carried out at low concentration MWCNTs or without MWCNTs membranes due to the effect of MIBK which acts as a pore former with large pore size in the polymer matrix [4,34]. MWCNTs improve the trans-membrane flux of PP composite membrane with 5 mg/g MWCNTs which gave the highest trans-membrane flux (45.95 L/m^2 h) [29]. Further increasing in the MWCNTs concentration, the VEDCMD permeate flux decreased due to the consequent decreasing in pore size.

3.2.4. Application of the synthesized MWCNTs/PP nano-composite membrane for oil field effluent water desalination

The oil field effluent water contain large amounts of inorganic salts, heavy metals, and naturally occurring radioactive material are of particular environmental concern [35] so the desalination of oil field

Table 3
The effect of polymer concentration on trans-membrane flux

Polymer concentration (wt.%)	Trans-membrane flux (L/m^2 h)
5.0	10.71
3.7	17.28
3.0	23.85
2.5	28.43
1.9	Rejected result*

*Due to the feed water passed through the membrane from the beginning of the test.

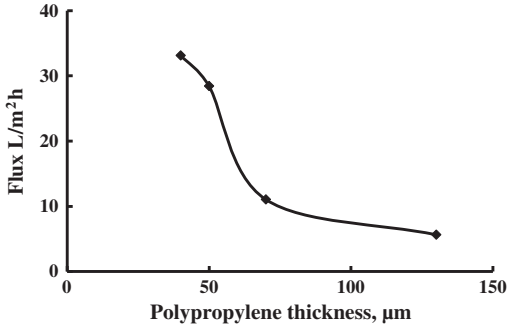

Fig. 11. Effect of poly propylene membrane thickness on trans-membrane flux.

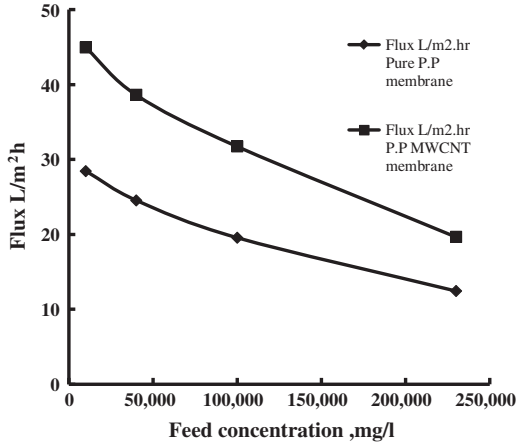

Fig. 12. The effect of feed concentration on the two types of membranes.

Table 4
The effect of MWCNTs concentrations on trans-membrane flux

Type of membrane	Flux L/m^2 h
Without CNT	Rejected result*
2 mg/g CNT	Rejected result*
5 mg/g CNT	45.95
10 mg/g CNT	35.71
20 mg/g CNT	28.31

*Due to the feed water passed through the membrane from the beginning of the test.

effluent water can potentially protect the environment and will provide a new source of water.

From the aforementioned studies to the performance of different synthesized membranes, two membranes are selected for the desalination of oil field effluent water, the first membrane was neat PP, while the second was MWCNTs/PP nano-composite membrane with 5 mg/gm. The thickness of both membranes was 50 µm with polymer concentration 2.5 wt.%. The experiments were tested at hot side temperature 55C, hot side flow rate 12 l/min, and cold side flow rate was 6 L/min.

Fig. 12 shows the performance of the two membranes on different four feed water samples, the first three samples were synthesized saline water with different salt concentration 10,000, 40,000, and 100,000 ppm, respectively, where the forth sample was the oil field effluent water sample with salt concentration 230,000 ppm.

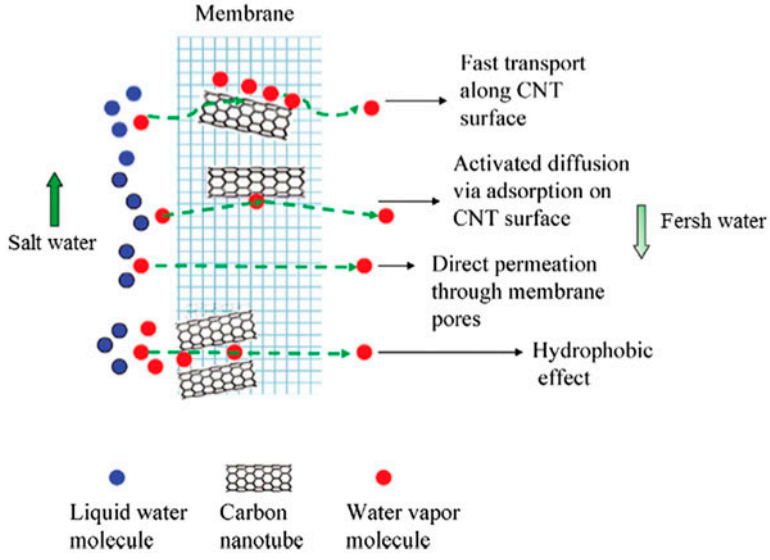

Fig. 13. A schematic diagram for separation mechanism of the synthesized MWCNTs/PP nano-composite membrane.

Table 5
A comparison between the current study and previous studies

Membrane	Method of membrane distillation	Operating conditions			Flux L/m^2 h	References
		Feed concentration ppm	Feed temperature ℃	Permeate temperature ℃		
Fluorinated hydrocarbon	VEDCMD	10,000	82	20	19	[17]
PTFE	VEDCMD	17,500	60	20	37.5	[15]
PVDF	DCMD	30,000	80	20	38.8	[25]
CNIM* on PP support	DCMD	10,000	70	15	36.8	[39]
MWCNT/PVDF	DCMD	35,000	82	20	34.2	[29]
Current study	VEDCMD	10,000	55	15	45.9	
	VEDCMD	40,000	55	15	38.6	
	VEDCMD	100,000	55	15	31.7	
	VEDCMD	230,000	55	15	19.6	

*CNIM is carbon nanotube immobilized membrane.

From Fig. 12 we can find that when neat PP membrane used for the oil field effluent water desalination, the flux was 12.43 L/m^2 h, however, when MWCNTs/PP nano-composite membrane used the flux was 19.66 L/m^2 h.

It is obvious that, the MWCNTs enhanced the performance of VEDCMD with 58% at the same operating conditions [39]. The results also show that the increase of feed solute concentration results in a reduction of the DCMD permeate flux. This behavior is attributed to the decrease of the water vapor pressure, the driving force, with the addition of non-volatile solute in water due to the decrease in water activity in the feed [21,38].

Fig. 13 shows a schematic diagram for separation mechanism of the synthesized MWCNTs/PP nano-composite membrane. The figure illustrates very high transport of water molecules inside the CNTs and their potential to change the water–membrane interaction to stop the permeation of liquid water molecules while favoring the preferential transport of vapors through the pores have encouraged their incorporation into the membrane matrix. [37,40].

3.3. Comparison with other MD membranes

Table 5 lists performance comparison between the current work and the previous investigations. It can be observed that the obtained data in this study are comparable or even better than most of the previous reports. Higher data obtained in Ref. [25] may be attributed to the higher feed temperature (80℃), and lower feed concentration 30,000 ppm.

4. Conclusions

An experimental study of vacuum-advanced direct contact membrane distillation (VEDCMD) process was carried out to desalinate the brine oil field produced water. The improvement of PP membrane was achieved through blending of multi-wall carbon nanotubes (MWCNTs) to the polymer matrix. This improvement was carried out to adjust the pore size.

The results showed that by decreasing the polymer concentration, the pore size increased and the flux increases until specific concentration under which pore-wetting phenomena occurs due to formation of large pore size. The membrane thickness has a negative influence on the VEDCMD flux where the increase of membrane thickness makes decline in trans-membrane flux. There is a positive influence of the feed temperature and the feed rate on the flux. On the other hand, there is a negative influence of the feed water concentration on the flux.

The addition of MWCNTs to the polypropylene membranes to form a nano-composite structure increase the surface roughness, i.e. increase the surface area and improve DCMD performance through preventing the pore-wetting phenomenon, thus, enhance the permeate flux.

Acknowledgments

It is a pleasure to acknowledge the financial support provided by the Science and Technological Development Fund (STDF) in Egypt through Grant 5240 (Egyptian Desalination Research Center of Excellence).

References

[1] F.R. Ahmadun, A. Pendashteh, L.C. Abdullaha, D.R.A. Biak, S.S. Madaeni, Z.Z. Abidin, Review of technologies for oil and gas produced water treatment, J. Hazard. Mater. 170 (2009) 530–551.

[2] "Law Number 9 of 2009", Promulgating the Environment Law and its Executive Regulation Egypt.

[3] J. Kucera, Desalination Water from Water, John Wiley and Scrivener Publishing LLC, Hoboken, NJ, Salem, Massachusetts, 2014.

[4] M. Khayet, T. Matsuura, Membrane Distillation: Principles and Applications, Elsevier, Amsterdam, the Netherlands, 2011.

[5] J. Woods, J. Pellegrino, J. Burch, Generalized guidance for considering pore-size distribution in membrane distillation, J. Membr. Sci. 368 (2011) 124–133.

[6] P. Wang, T. Chung, Recent advances in membrane distillation processes: Membrane development, configuration design and application exploring, J. Membr. Sci. 474 (2015) 39–56.

[7] A.E. Jansen, J.W. Assink, J.H. Hanemaaijer, J. van Medevoort, E. van Sonsbeek, Development and pilot testing of full-scale membrane distillation modules for deployment of waste heat, Desalination 323 (2013) 55–65.

[8] E. Drioli, A. Ali, F. Macedonio, Membrane distillation: Recent developments and perspectives, Desalination 356 (2015) 56–84.

[9] M.M.A. Shirazi, A. Kargari, M. Tabatabaei, Evaluation of commercial PTFE membranes in desalination by direct contact membrane distillation, Chem. Eng. Process. 76 (2014) 16–25.

[10] L. García-Fernández, M.C. García-Payo, M. Khayet, Effects of mixed solvents on the structural morphology and membrane distillation performance of PVDF-HFP hollow fiber membranes, J. Membr. Sci. 468 (2014) 324–338.

[11] Ó. Andrjesdóttir, C.L. Ong, M. Nabavi, S. Paredes, A.S.G. Khalil, B. Michel, D. Poulikakos, An experimentally optimized model for heat and mass transfer in direct contact membrane distillation, Int. J. Heat Mass Transfer 66 (2013) 855–867.

[12] Y. Tang, N. Li, A. Liu, S. Ding, C. Yi, H. Liu, Effect of spinning conditions on the structure and performance of hydrophobic PVDF hollow fiber membranes for membrane distillation, Desalination 287 (2012) 326–339.

[13] M.M.A. Shirazi, A. Kargari, M.J.A. Shirazi, Direct contact membrane distillation for seawater desalination, Desalin. Water Treat. 49(1–3) (Nov. 2012) 368–375.

[14] Z.-Q. Dong, X.-H. Ma, Z.-L. Xu, W.-T. You, F.-B. Li, Superhydrophobic PVDF–PTFE electrospun nanofibrous membranes for desalination by vacuum membrane distillation, Desalination 347 (2014) 175–183.

[15] C.R. Martinetti, A.E. Childressa, T.Y. Cath, High recovery of concentrated RO brines using forward osmosis and membrane distillation, J. Membr. Sci. 331 (2009) 31–39.

[16] T.Y. Cath, V.D. Adams, A.E. Childress, Experimental study of desalination using direct contact membrane distillation: a new approach to flux enhancement, J. Membr. Sci. 228 (2004) 5–16.

[17] J. Zhang, J.-D. Li, M. Duke, Z. Xie, S. Gray, Performance of asymmetric hollow fibre membranes in membrane distillation under various configurations and vacuum enhancement, J. Membr. Sci. 362 (2010) 517–528.

[18] M.C. García-Payo, M. Essalhi, M. Khayet, Effects of PVDF-HFP concentration on membrane distillation performance and structural morphology of hollow fiber membranes, J. Membr. Sci. 347 (2010) 209–219.

[19] G. Naidu, Y. Choi, S. Jeong, T.M. Hwang, S. Vigneswaran, Experiments and modeling of a vacuum membrane distillation for high saline water, J. Ind. Eng. Chem. 20 (2014) 2174–2183.

[20] J. Minier-Matar, A. Hussain, A. Janson, F. Benyahia, S. Adham, Field evaluation of membrane distillation technologies for desalination of highly saline brines, Desalination 351 (2014) 101–108.

[21] H.J. Hwang, K. He, S.Gray, J. Zhang, I.S. Moon, Direct contact membrane distillation (DCMD): Experimental study on the commercial PTFE membrane and modeling, J. Membr. Sci. 371 (2011) 90–98.

[22] Z. Li, Y. Peng, Y. Dong, H. Fan, P. Chen, L. Qiu, Q. Jiang, Effects of thermal efficiency in DCMD and the preparation of membranes with low thermal conductivity, Appl. Surf. Sci. 317 (2014) 338–349.

[23] D. Singh, K.K. Sirkar, Desalination of brine and produced water by direct contact membrane distillation at high temperatures and pressures, J. Membr. Sci. 389 (2012) 380–388.

[24] S. Lin, N.Y. Yip, M. Elimelech, Direct contact membrane distillation with heat recovery: Thermodynamic insights from module scale modeling, J. Membr. Sci. 453 (2014) 498–515.

[25] M. Essalhi, M. Khayet, Self-sustained webs of polyvinylidene fluoride electrospun nano-fibers: Effects of polymer concentration and desalination by direct contact membrane distillation, J. Membr. Sci. 454 (2014) 133–143.

[26] M. Khayet, Membranes and theoretical modeling of membrane distillation: A review, Adv. Colloid Interface Sci. 164(1–2) (May 2011) 56–88.

[27] Y.M. Manawi, M.A.M.M. Khraisheh, A.K. Fard, F. Benyahia, S. Adham, A predictive model for the assessment of the temperature polarization effect in direct contact membrane distillation desalination of high salinity feed, Desalination 341 (2014) 38–49.

[28] S.S. Madaeni, S. Zinadini, V. Vatanpour, Preparation of superhydrophobic nanofiltration membrane by embedding multiwalled carbon nanotube and polydimethylsiloxane in pores of microfiltration membrane, Sep. Purif. Technol. 111 (2013) 98–107.

[29] T.L.S. Silva, S. Morales-Torres, J.L. Figueiredo, A.M.T. Silva, Multi-walled carbon nanotube/PVDF blended membranes with sponge- and finger-like pores for direct contact membrane distillation, Desalination 357 (2015) 233–245.

[30] L. Dumée, V. Germain, K. Sears, J. Schütz, N. Finn, M. Duke, S. Cerneaux, D. Cornu, S. Gray, Enhanced durability and hydrophobicity of carbon nanotube bucky paper membranes in membrane distillation, J. Membr. Sci. 376(1–2) (2011) 241–246.

[31] T. Kitano, Y. Maeda, T. Akasak, Preparation of transparent and conductive thin films of carbon nanotubes

using a spreading/coating technique, Carbon 47(15) (December 2009) 3559–3565.
[32] V. Ambrogia, G. Gentile, C. Ducati, M.C. Oliva, C. Carfagna, Multiwalled carbon nanotubes functionalized with maleated poly(propylene) by a dry mechanochemical process, Polymer 53 (2012) 291–299.
[33] H.A. Shawky, S.R. Chae, S. Lin, M.R. Wiesner, Synthesis and characterization of a carbon nanotube/polymer nanocomposite membrane for water treatment, Desalination 272 (2011) 46–50.
[34] J.A. Franco, S.E. Kentish, J.M. Perera, G. Stevens, Fabrication of a superhydrophobic polypropylene membrane by deposition of a porous crystalline polypropylene coating, J. Membr. Sci. 318 (2008) 107–113.
[35] J. Neff, K. Lee, E.M. De Blois, Produced Water: Overview of Composition, Fates, and Effects, Springer, New York, NY, 2011.
[36] Y. Mansourpanah, S.S. Madaeni, A. Rahimpour, M. Adeli, M.Y. Hashemi, M.R. Moradian, Fabrication new PES-based mixed matrix nanocomposite membranes using polycaprolactone modified carbon nanotubes as the additive: Property changes and morphological studies, Desalination 277 (2011) 171–177.
[37] L. Dumée, J.L. Campbe, K. Sears, J. Schütz, N. Finn, M. Duke, S. Gray, The impact of hydrophobic coating on the performance of carbon nanotube bucky-paper membranes in membrane distillation, Desalination 283 (2011) 64–67.
[38] D. Winter, J. Koschikowski, S. Ripperger, Desalination using membrane distillation: Flux enhancement by feed water deaeration on spiral-wound modules, J. Membr. Sci. 423–424 (Dec. 2012) 215–224.
[39] S. Roy, M. Bhadra, S. Mitra, Enhanced desalination via functionalized carbon nanotube immobilized membrane in direct contact membrane distillation, Sep. Purif. Technol. 136 (2014) 58–65.
[40] K. Gethard, O. Sae-Khow, S. Mitra, Water desalination using carbon-nanotubeenhanced membrane distillation, ACS Appl. Mater. Interfaces 3 (2011) 110–114.